Separation Science and Technology
Publication details, including instructions for authors and subscription information:
http://www.informaworld.com/smpp/title~content=t713708471

A Novel Continuous Rotating Annular Liquid Chromatograph with a Multichannel Peristaltic Pump for Variable Eluent Withdrawal

Toshikuni Yonemoto[a]; Akio Kitakawa[a]; Shuang Ning Zheng[a]; Teiriki Tadaki[a]
[a] DEPARTMENT OF BIOCHEMISTRY AND ENGINEERING, TOHOKU UNIVERSITY, SENDAI, JAPAN

To cite this Article Yonemoto, Toshikuni , Kitakawa, Akio , Zheng, Shuang Ning and Tadaki, Teiriki(1993) 'A Novel Continuous Rotating Annular Liquid Chromatograph with a Multichannel Peristaltic Pump for Variable Eluent Withdrawal', Separation Science and Technology, 28: 17, 2587 — 2605
To link to this Article: DOI: 10.1080/01496399308017498
URL: http://dx.doi.org/10.1080/01496399308017498

SEPARATION SCIENCE AND TECHNOLOGY, **28**(17&18), pp. 2587–2605, 1993

A Novel Continuous Rotating Annular Liquid Chromatograph with a Multichannel Peristaltic Pump for Variable Eluent Withdrawal

TOSHIKUNI YONEMOTO,* AKIO KITAKAWA,
SHUANG NING ZHENG, and TEIRIKI TADAKI
DEPARTMENT OF BIOCHEMISTRY AND ENGINEERING
TOHOKU UNIVERSITY
AOBA, ARAMAKI, AOBA-KU, SENDAI 980, JAPAN

ABSTRACT

A novel continuous rotating annular chromatograph is proposed and used for the separation of amino acids. The system is equipped with a multichannel peristaltic pump to withdraw the eluent and to easily regulate its flow rate. The inlet of the annular chromatographic packed bed is divided into a number of chambers to prevent circumferential dispersion of the sample. The mass transfer characteristics of the apparatus were theoretically analyzed by using a two-dimensional transport model. The experimental results for solute elution are well simulated by the transport model. Solute dispersion in the annular column was found to be negligible. A shallower liquid depth in the inlet chamber gave sharper concentration peaks. An increase in the number of feed nozzles and the installation of inlet chambers were found to be preferable for multicomponent separation.

INTRODUCTION

A continuous rotating annular chromatograph (CRAC) proposed by Martin (1), Giddings (2), and Fox et al. (3–5) and modified by several groups (6–10) has future potential for use in large-scale separation of a variety of biological compounds such as amino acids and proteins.

* To whom correspondence should be addressed. Telephone: 81-22-222-1800. FAX: 81-22-268-2948.

Martin (1) was first to propose the idea of continuous chromatographic separation using a rotating annular apparatus.

Giddings (2) made a theoretical analysis of the performance of CRAC using a plate theory. He predicted that CRAC will be potentially capable of greater throughput than a large conventional column of similar cross section.

One of the original versions prepared by Fox et al. (3–5) is filled with effluent at a fixed level over chromato-resin packing. The flow rate of the eluent in the packed bed can be regulated by changing the liquid level of the eluent. The sample liquid, which contains solutes to be separated, is fed into a effluent liquid at a point just above the packing. The apparatus was used to purify bovine myoglobin and to isolate several proteins from skim milk.

Begovich et al. (6, 7) provided another means of regulating the eluent flow rate. Sealing the supply section enables their apparatus to arbitrarily supply pressurized effluent. They investigated the effect of such operating variables as sample and eluent feed rates, sample concentration, and the rotation rate of the tower on the resolving power.

Goto et al. (8) proposed a new apparatus with a stationary heavy annular bed, rotating light feed nozzle, and product collector. The bottom end of the nozzle is immersed in the packed bed to prevent solute dispersion along the circumferential direction above the packing. Their apparatus has almost the same resolving power as that of a conventional batchwise column chromatograph.

Recently, Carta et al. (9) and Hashimoto et al. (10) carried out the continuous separation of biological compounds using the same type of rotating annular chromatograph as that of Fox et al. (3). A metering pump and liquid level controller were used for regulation of the flow rate by Carta et al. and Hashimoto et al., respectively. Dispersion above the packing was prevented in both apparatuses by immersing the sample nozzle into the packing in the same manner as in Goto's apparatus. Hashimoto et al. observed that the resolving power decreases with increasing eluent flow rate. They attributed the low resolving power to turbulent convection in the packing and emphasized the necessity of improving the structure of the feed nozzle tip to minimize the turbulent convection.

The achievement of plug flow in the column is essential for the chromatograph to have a high resolving power. The supply of sample feed must not disturb the eluent flow in the column. The ability to set the eluent flow rate arbitrarily is required so the optimum operating conditions can be found.

Gravity forces the eluent to flow down the columns in most of the previously developed apparatuses other than Begovich's. The variation

in the eluent flow rate is limited to a small range even if a liquid level control unit is located at the column inlet. Pressurized operation overcomes this disadvantage, but the apparatus is complex and expensive.

In this paper a new CRAC which eliminates the above-mentioned disadvantages is proposed. The apparatus is equipped with a multichannel peristaltic pump at the outlet of the annular column to withdraw the eluent and to regulate its flow rate over a wide range. Separation experiments of two amino acids were performed to show the effectiveness of the apparatus. The mass transfer characteristics have also been analyzed by using a two-dimensional transport model and single solute dispersion experiments.

CONSTRUCTION OF A NEW CONTINUOUS ROTATING ANNULAR CHROMATOGRAPHIC APPARATUS

The new CRAC has the following features.

1. A 36-channel peristaltic pump is situated at the outlet of the column to withdraw the eluent and to regulate its flow rate over a wide range.
2. The pump is set on a pedestal which revolves on the center axis of the annular chromatographic column in order to avoid leakage of eluent at the junction between the column and the pump.
3. Another 36-channel peristaltic pump is used for supplying eluent and feeding the sample to the top of the column.
4. The inlet of the annular column is divided into a number of chambers to prevent circumferential dispersion of the sample mixture before it enters the column.

Conceptual and detailed figures are shown in Figs. 1 and 2, respectively. The apparatus consists of four sections: the feed supply, separation tower, liquid recovery, and driving unit. The annular chromatographic separation tower rotates, while the liquid supply and recovery units are fixed, as in Fox's apparatus.

Thirty-six stainless steel tubes of 50 mm length, 2 mm outer diameter, and 1 mm inner diameter are set into a fixed acrylic resin disk in concentric circles and connected to the peristaltic pump (Ismatec Sa., MV-MS6/CA8) to serve as the feed supply nozzles.

The annular separation tower is made of acrylic resin and measures 470 mm in length, 160 mm o.d., and 150 mm i.d. Cation-exchange resin with an average diameter of 0.22 mm (Mitsubishi Kasei Co., DIAION-UBK530) is packed into the annular slit to allow the tower to act as a chromatographic device.

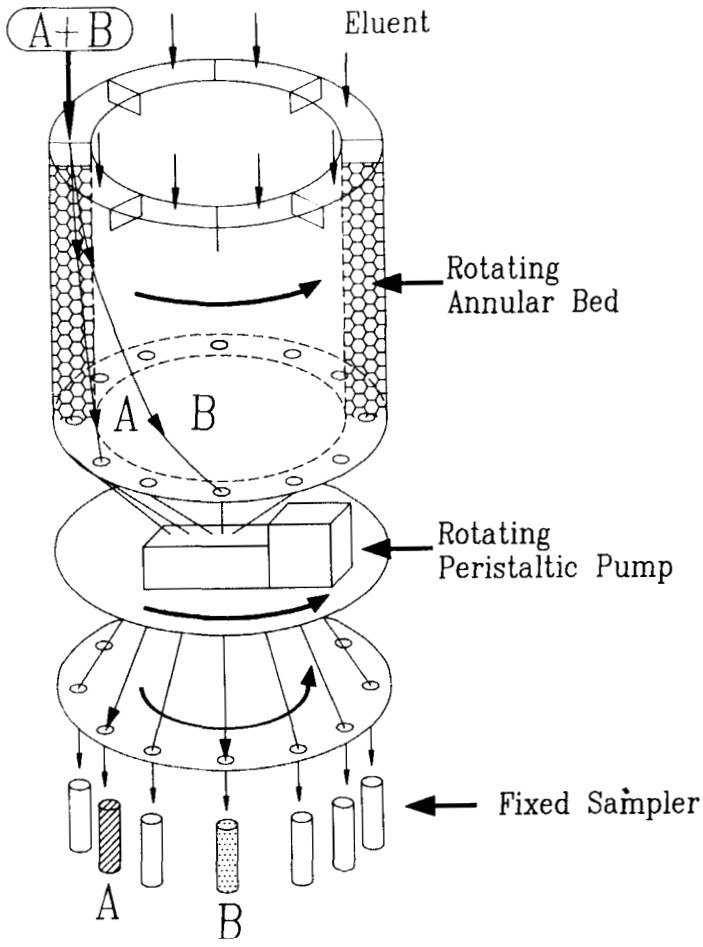

FIG. 1 Concept of continuous rotating annular chromatograph with multichannel peristaltic pump.

Thirty-six acrylic resin plates of 1 mm thickness are used as partitions between the chambers at the annular inlet, as shown in the upper right corner of Fig. 2. Thirty-six stainless steel tubes of 2 mm o.d. and 1 mm i.d. are inserted at the bottom of the annular column to serve as liquid withdrawal ports. The mouth of each tube is plugged with glass wool to prevent resin from falling into the tubes. Each tube is connected with another peristaltic pump for the withdrawal via a 0.8-mm i.d. silicon tube.

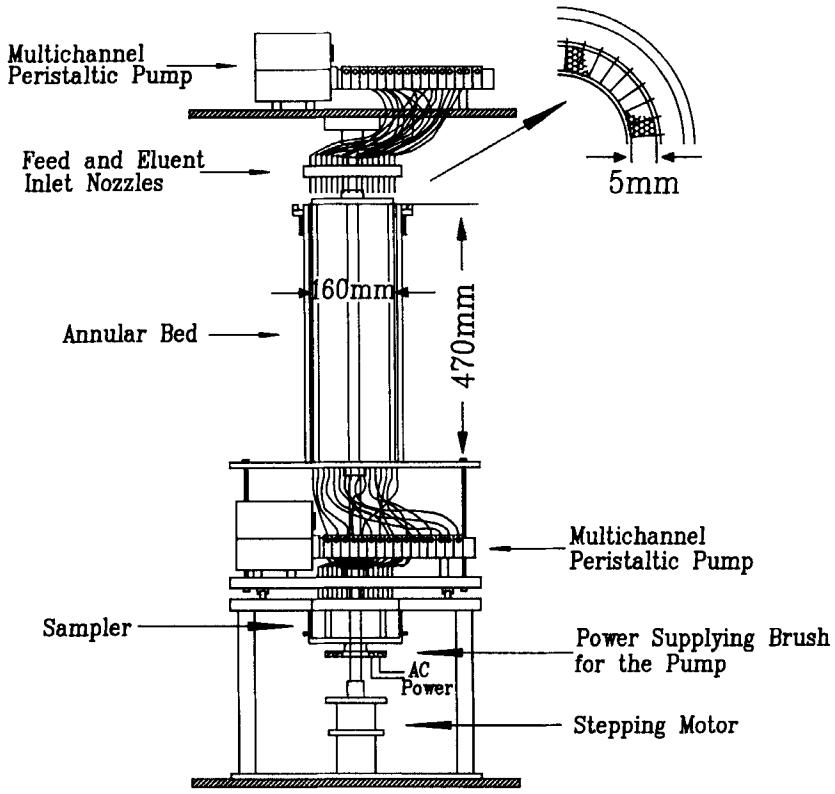

FIG. 2 Detail of continuous rotating annular chromatograph with 36-channel peristaltic pump.

Identical multichannel peristaltic pumps are used for the feed supply and liquid withdrawal. A slight excess of feed is supplied to the inlet chamber, and the excess is forced to overflow from the chamber into the drain arranged on the outside of the column in order to prevent the packed resin from drying out caused by any fluctuations in the pumping rate of the two pumps.

The annular chromatographic tower and the pump for liquid withdrawal are set on a mobile disk 640 mm in diameter and made of 15 mm thick stainless steel. The disk has four wheels and rotates at a steady fixed velocity on a stationary disk by receiving torque from a 5-phase stepping motor (Oriental Motor Co., UPD566A). Thirty-six stainless steel tubes of 2 mm o.d. and 1 mm i.d. connected to the peristaltic pump are set into a

mobile disk in concentric circles and serve as a liquid outlet. The liquid that drops from the tubes is collected by 36 stationary containers arranged continuously in concentric circles.

Phosphor bronze brushes are used for power supply to the rotating pump for liquid withdrawal. A microcomputer (NEC, PC9801F) and a digital I/O board (Neolog Electric Co., PCN-1098) are used for control of the stepping motor.

EXPERIMENTAL PROCEDURE

A mixed solution of glutamic acid (pI = 3.22) and valine (pI = 5.96) was used as a sample for separation experiments. The concentration of each amino acid was 10 mol/m^3. Ten mol/m^3 sodium acetate buffer solution (pH = 5.0) was used as the eluent. About 10% of the valine was positively charged and the remainder was uncharged; whereas about 10% of the glutamic acid was uncharged and the remainder was negatively charged. Valine has a stronger affinity for the cation-exchange resin at this pH condition; therefore it might be eluted at a larger angle compared with glutamic acid.

The dispersion of the solute in the apparatus was investigated by allowing the resin to function as inert packing. An aqueous solution of 10 mol/m^3 glutamic acid was used as the sample liquid and a buffer solution of 10 mol/m^3 sodium phosphate (pH = 7.5) was used as the eluent. More than 99% of the glutamic acid was negatively charged under this pH condition. Any chemical interaction between the cation-exchange resin and glutamic acid was practically negligible.

The amino acid sample and eluent solution were first supplied continuously by using the peristaltic pump, while another pump for liquid withdrawal was then allowed to operate at a fixed flow rate (97% of the feed flow rate). The annular column was also allowed to rotate at a fixed revolving rate.

After attaining steady-state, the outlet eluents were collected and subjected to quantitative analysis by a fluorescence spectrophotometer (Hitachi Co., F-1050), using the *o*-phthalaldehyde method to determine the solute concentrations.

All chemicals used were of special grade and were purchased from Wako Pure Chemical Industries.

MATHEMATICAL ANALYSIS FOR SOLUTE DISPERSION

Consider an annular rotating packed bed in which the dimension of the annular slit thickness is much smaller than that of the annular column

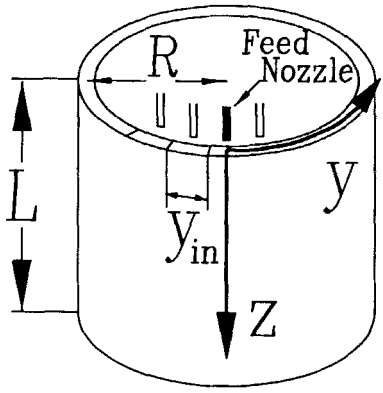

FIG. 3 Coordinate system.

radius. Two-dimensional rectangular coordinates instead of cylindrical coordinates can then be used to derive mathematical equations. The y-axis and z-axis corresponding to the circumferential and axial directions, respectively, are set as shown in Fig. 3.

The inlet part of the packed bed is schematically shown in Fig. 4. The inlet of the annular column is divided into 36 chambers where liquid is stored at a depth of 10 mm, similar to the experimental apparatus. The sample and eluent solutions from the nozzles pass through the chambers

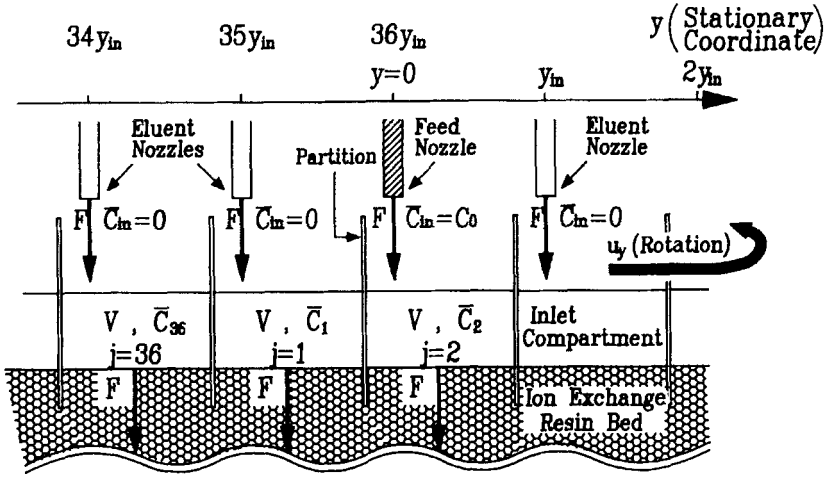

FIG. 4 Schematic diagram of inlet of continuous rotating annular packed bed.

and then flow into the annular packed bed. The rotation of the annular bed causes a periodic concentration change in the solute in the chamber.

Assuming the chambers to be in a state of perfect mixing, let us first derive the solution for the concentration in the inlet chambers into which a sample solution is fed from one feed nozzle and the eluent from the other nozzles. The periodic solution is obtained analytically by means of several mathematical treatments (see Eqs. A-1–A-9 in the Appendix).

If the periodic solution for the concentration in the inlet chamber is used for the inlet boundary condition, the concentration in the annular packed bed also varies periodically. It is obvious from Eqs. (A-1)–(A-9) in the Appendix, however, that the time variation of the chamber concentration is decreasing faster than the positional variation along the y-axis as the number of chambers increases.

To simplify the analysis, the time average value of the concentration in the chamber is used for the inlet boundary condition of the packed bed (see the Appendix). The boundary equations are:

$$\frac{C_y}{C_0} = \frac{y_{in} - y}{y_{in}} + \frac{1}{\Theta}\left[\alpha\left\{\exp(-\Theta) - \exp\left(-\Theta\frac{y}{y_{in}}\right)\right\} - \{1 - \alpha\exp(-\Theta)\}\left\{\exp\left(-\Theta\frac{y}{y_{in}} - 1\right)\right\}\right] \qquad (0 < y \leq y_{in}) \quad (1a)$$

$$\frac{C_y}{C_0} = \frac{1}{\Theta}\left([\exp\{-(j-1)\Theta\} - \alpha\exp(-j\Theta)] \times \left[1 - \exp\left\{-\Theta\frac{y - (j-1)y_{in}}{y_{in}}\right\}\right] + [\exp\{-(j-2)\Theta\} - \alpha\exp\{-(j-1)\Theta\}] \times \left[\exp\left\{-\Theta\frac{y - (j-1)y_{in}}{y_{in}}\right\} - \exp(-\Theta)\right]\right) \qquad ((j-1)y_{in} < y \leq jy_{in}, j = 2, 3, \ldots, 35) \quad (1b)$$

$$\frac{C_y}{C_0} = \frac{y - 35y_{in}}{y_{in}} + \frac{1}{\Theta}\left[\alpha\left\{\exp\left(-\Theta\frac{y - 35y_{in}}{y_{in}}\right) - 1\right\} - \{\exp(-34\Theta) - \alpha\exp(-35\Theta)\}\left\{\exp(-\Theta) - \exp\left(-\Theta\frac{y - 35y_{in}}{y_{in}}\right)\right\}\right] \qquad (35y_{in} < y \leq 36y_{in}) \quad (1c)$$

Because no affinity exists between the cation-exchange resin in the packed bed and the solute amino acid in substance, the steady-state mass balance can be expressed as

$$E_z \frac{\partial^2 C}{\partial z^2} - u_z \frac{\partial C}{\partial z} + E_y \frac{\partial^2 C}{\partial y^2} - u_y \frac{\partial C}{\partial y} = 0 \tag{2}$$

Here, E_z and E_y are dispersion coefficients for the respective directions. u_z is the interstitial fluid velocity in the bed, and u_y is the circumferential velocity of the annular slit.

Using a closed vessel approximation in the exit of the packed bed gives the following exit boundary condition:

$$\partial C/\partial z = 0 \qquad \text{at} \qquad z = L \tag{3}$$

By considering periodic continuity, the circumferential boundary conditions are given as follows:

$$C(y = 0) = C(y = 2\pi R) \tag{4}$$

$$\left.\frac{\partial C}{\partial y}\right|_{y=0} = \left.\frac{\partial C}{\partial y}\right|_{y=2\pi R} \tag{5}$$

These formulas are a set of governing equations and can be solved by means of the finite-difference numerical method. The numbers of the finite-difference grids are, respectively, 2000 for the z-axis and 1500 for the y-axis.

The dispersion coefficients are estimated by the Ligny–Giddings' equation (11).

RESULTS AND DISCUSSION

Separation of Two Solutes

Figure 5 shows a typical experimental result for the separation of two solutes. The sample containing two amino acids was supplied from one nozzle and the eluent adjusted to pH 5.0 was supplied from all the other nozzles. The number on the abscissa corresponds to the stationary container for liquid recovery numbered from just beneath the sample nozzle in the same direction as the rotation. Valine had a much larger affinity for the cation-exchange resin at this pH than did glutamic acid. That was why valine was retained longer in the column and eluted at a large numbered position for liquid recovery and why the separation of two solutes was attained. The peak shape for the valine elution was quite broad. Nonisocratic elution along the angular position might be required for sharper elution; however, further discussion will not be conducted here.

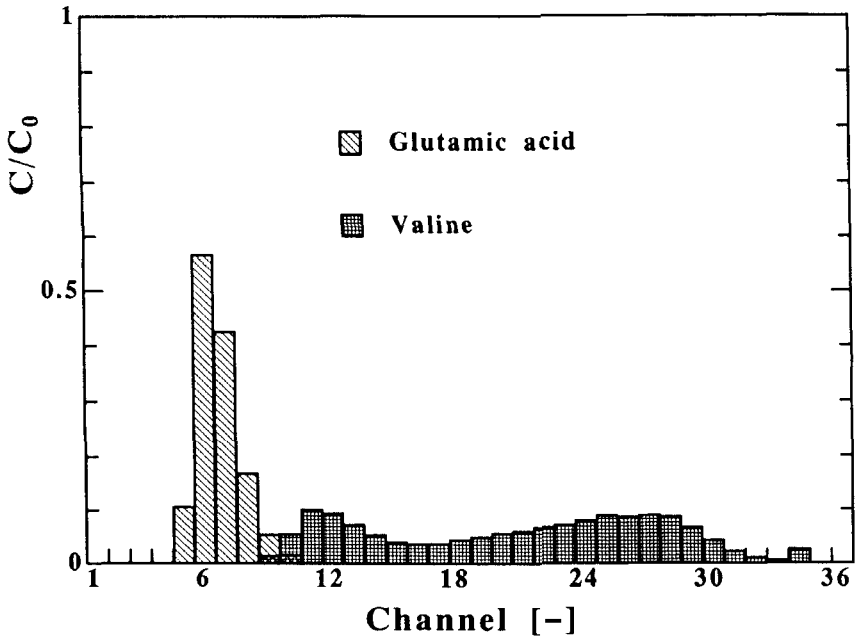

FIG. 5 Elution profile of glutamic acid and valine. Residence time = 400 seconds, rotation speed = 0.1 deg/s, and eluent pH 5.0.

Effect of Residence Time in the Annular Bed on Solute Dispersion

Figures 6 and 7 show the concentration distribution of solute in the outlet of the column. Glutamic acid was used as the solute. The pH of the eluent was 7.5, and more than 99% of the glutamic acid was negatively charged at this pH; hence, interaction between the solute and the resin was virtually absent. The transport characteristics could then be elucidated. The time-average distribution of solute concentration in the annular column inlet is represented by the dotted curve. There was a restriction of the number of inlet chambers; therefore, the peak was not as sharp. Glutamic acid concentrations obtained experimentally from the liquid recovering containers are represented by the plots with filled circles. Dashed and solid lines indicate calculated results, taking Ligny–Giddings' dispersion coefficients into account and setting dispersion coefficients to zero. Integral average values with respect to each channel width obtained from

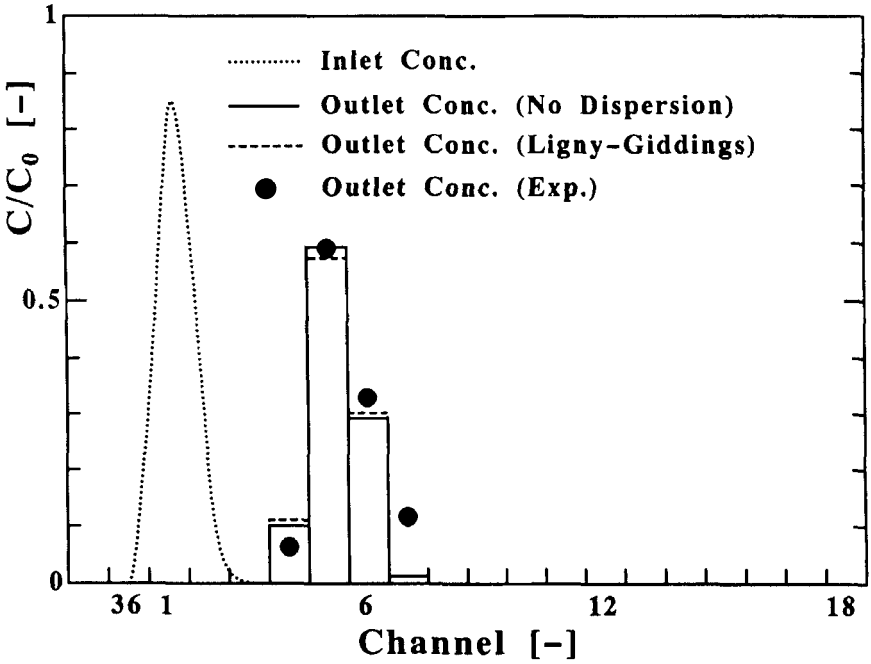

FIG. 6 Inlet and outlet concentration distribution. Residence time = 400 seconds and rotation speed = 0.1 deg/s. The dashed line is not evident because its position is almost the same as that of the solid line.

the following equation were adopted for theoretical results:

$$\frac{\overline{C}}{C_0} = \frac{\int_{jy_{in}}^{(j+1)y_{in}} \frac{C}{C_0}\, dy}{\int_{jy_{in}}^{(j+1)y_{in}} dy} \tag{6}$$

The theoretical results both with and without solute dispersion were in excellent agreement with the experimental results for the two residence time conditions. This suggests that the model and numerical calculation are valid and also suggests that there exists only convective transport in the column in substance. It is also understandable by a detailed comparison of the two figures that a smaller residence time corresponds to a larger superficial velocity and gives a sharper peak of the elution curve at the smaller numbered position.

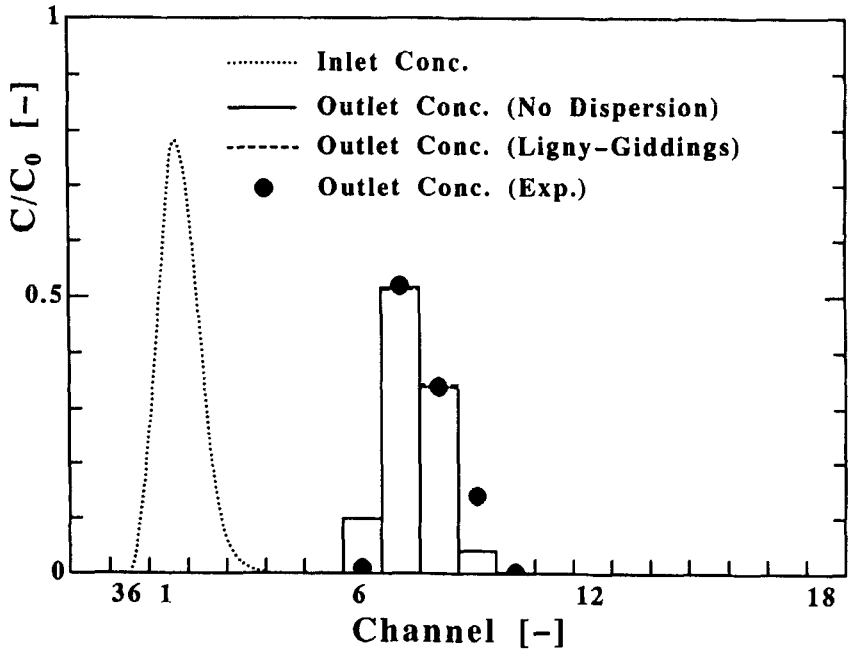

FIG. 7 Inlet and outlet concentration distribution. Residence time = 600 seconds and rotation speed = 0.1 deg/s. The dashed line is not evident because its position is almost the same as that of the solid line.

Effect of Rotation of the Annular Packed Bed

Figures 8 and 9 show the results for the 0.2 deg/s rotation condition. Compared with those in Figs. 6 and 7, broad peaks were observed for both the column inlet and outlet. The larger numbered positions of the outlet peaks can be considered to be suitable for the separation of two solutes which have similar affinities for the packed resin. Simulated values are in agreement with the experimental values within an allowable limit.

Effect of Liquid Depth in the Inlet Chambers

A liquid depth of 10 mm in the inlet chambers had been used in theoretical analyses to simulate the experiments. Let us now consider the effect of liquid depth on the concentration distribution at both the inlet and outlet of the packed bed. Substituting various liquid depths into Eq. (1) gives the results shown in Fig. 10. Numerical simulations were performed only in the case where no solute dispersion exists. It can be found from these

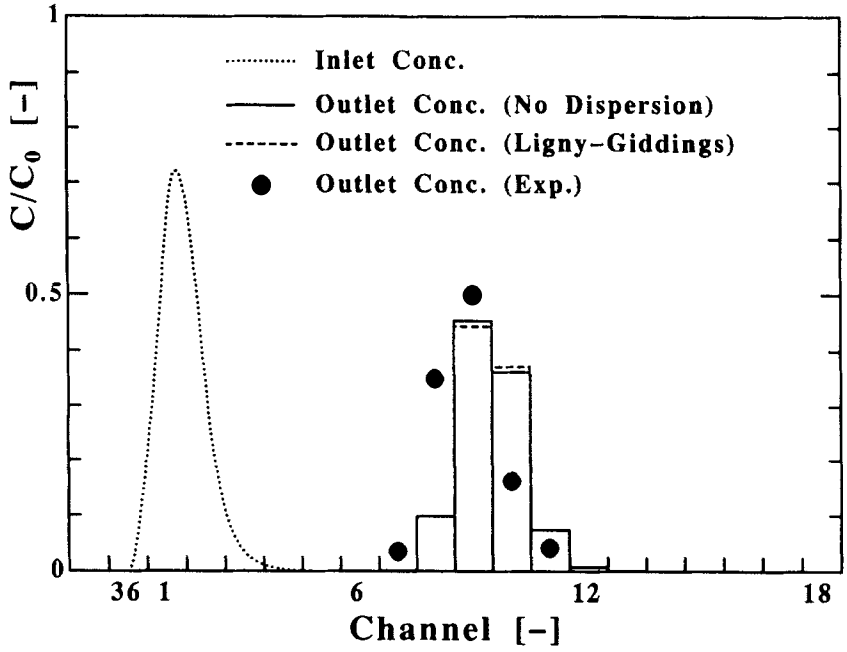

FIG. 8 Inlet and outlet concentration distribution. Residence time = 400 seconds and rotation speed = 0.2 deg/s. The dashed line is not evident because its position is almost the same as that of the solid line.

calculations that a shallower liquid depth gives a sharper concentration peak and is desirable for separation.

Effect of the Number of the Inlet Chambers and Feed Supply Nozzles

Thirty-six feed nozzles and an equal number of inlet chambers were equipped in the apparatus we prepared; however, more nozzles and chambers may be required for a commercial apparatus. To explore the effect of the number of chambers and nozzles, numerical simulations were performed for the cases where 72 and 144 inlet chambers were equipped at the column inlet. Solute concentrations supplied from one nozzle linearly increase with the number of the nozzles to keep the mass flow rate of the solute constant. The results are shown in Fig. 11. The higher the number, the sharper the distributions that can be attained for both the inlet and the outlet concentrations. It is clear that the increase in the number of

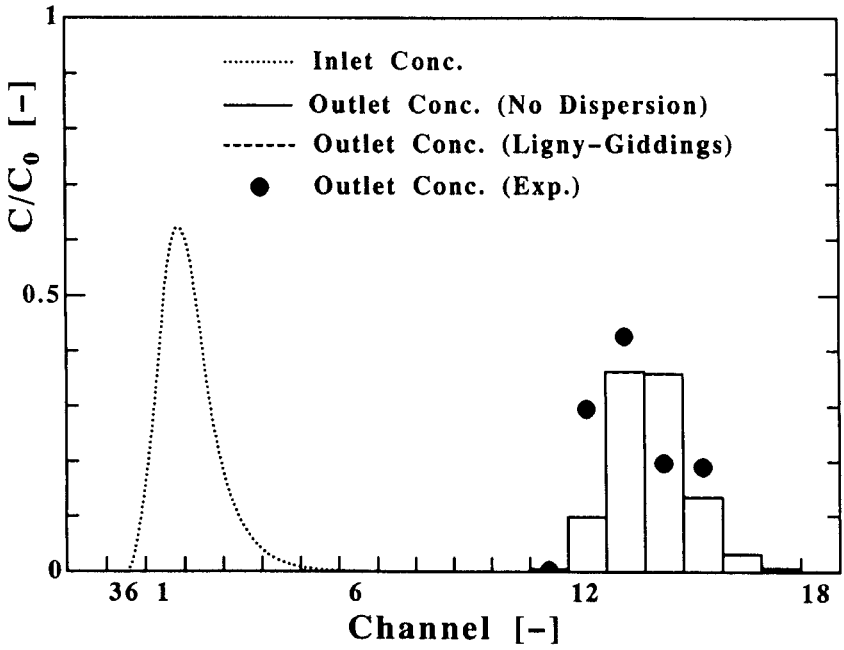

FIG. 9 Inlet and outlet concentration distribution. Residence time = 600 seconds and rotation speed = 0.2 deg/s. The dashed line is not evident because its position is almost the same as that of the solid line.

the feed nozzles and the installation of inlet chambers is preferable for multicomponent separation on an industrial scale.

CONCLUSIONS

A new type of continuous rotating annular chromatograph in which the flow rate is easily regulated over a wide range with no disturbance of eluent flow during supply of the sample feed has been proposed and used for the separation of amino acids. The transport characteristics have also been analyzed by using a two-dimensional transport model. The experimental and theoretical results show that:

1. Two amino acids can be separated by this CRAC.
2. Solute dispersion in the annular column can be neglected, and only convective transport exists under the operating conditions investigated.

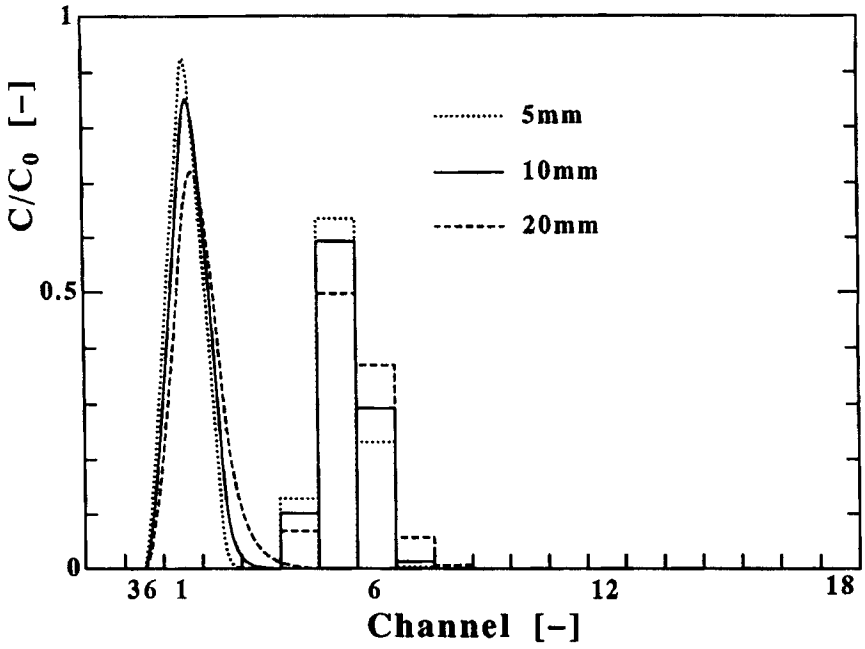

FIG. 10 Effect of liquid depth change in inlet chamber on concentration distribution at inlet and outlet of the packed bed. Residence time = 400 seconds and rotation speed = 0.1 deg/s.

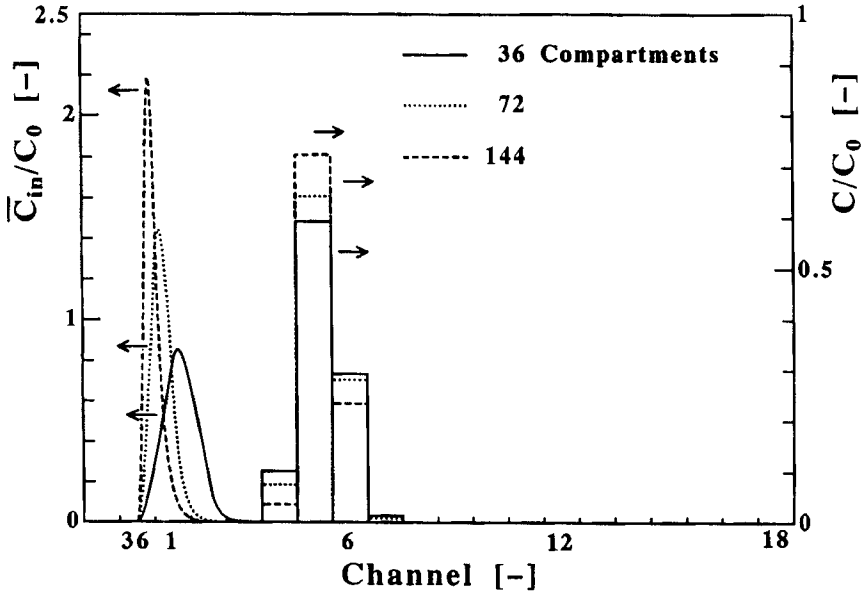

FIG. 11 Effect of inlet compartment number on inlet and outlet concentration. Residence time = 400 seconds and rotation speed = 0.1 deg/s.

3. Shallower liquid depth in the inlet chamber gives sharper concentration peaks and is desirable for separation.
4. An increase in the number of feed nozzles and the installation of inlet chambers is preferable for multicomponent separation.

APPENDIX: DERIVATION OF INLET BOUNDARY CONDITION

First consider the concentration change in the inlet chambers over the time interval $0 \leq t \leq y_{in}/u_y$ by setting the time at which the solute sample begins to flow into the first chamber at zero.

Using the perfect mixed vessel model, the following mass balance equation for the inlet chambers applies:

$$\tau \frac{d\overline{C_j}}{dt} = \overline{C_{in}} - \overline{C_j} \tag{A-1}$$

Here, $\overline{C_j}$ is the solute concentration in the jth chamber and τ ($\equiv V/F$) is the residence time in the chamber. $\overline{C_{in}}$ is the solute concentration in the feed from the nozzle. $\overline{C_{in}}$ is C_0 or zero for the respective feeds from the sample nozzle or eluent nozzle. Thus, for $0 \leq t \leq y_{in}/u_y$:

$$\overline{C_{in}} = C_0 \qquad (j = 1) \tag{A-2a}$$

$$= 0 \qquad (j = 2, 3, \ldots, 36) \tag{A-2b}$$

Solving Eqs. (A-1) and (A-2) yields

$$\overline{C_j} = C_0 - (C_0 - \overline{C_1}(0)) \exp\left(-\frac{t}{\tau}\right) \qquad (j = 1) \tag{A-3a}$$

$$= \overline{C_j}(0) \exp\left(-\frac{t}{\tau}\right) \qquad (j = 2, 3, \ldots, 36) \tag{A-3b}$$

Here, $\overline{C_j}(0)$ is the solute concentration in the jth chamber at $t = 0$.

The concentration in the jth chamber at $t = y_{in}/u_y$ is equal to that in the $(j + 1)$th chamber at $t = 0$; therefore, the following relationship can be set up over the time interval $y_{in}/u_y \leq t \leq 2y_{in}/u_y$:

$$\overline{C_j}(0) = \overline{C_{36}}(t_1) \qquad (j = 1) \tag{A-4a}$$

$$= \overline{C_{j-1}}(t_1) \qquad (j = 2, 3, \ldots, 36) \tag{A-4b}$$

Here, t_1 is equal to y_{in}/u_y.

Rearranging Eq. (A-3) by using (A-4) yields

$$\overline{C_j} = C_0 - \{C_0 - \overline{C_{36}}(t_1)\} \exp\left(-\frac{t}{\tau}\right) \qquad (j = 1) \tag{A-5a}$$

$$= C_0 \exp\{-(j-1)\Theta\} - \{C_0 - \overline{C_{36}}(t_1)\} \exp\{-(j-1)\Theta\} \exp\left(-\frac{t}{\tau}\right) \qquad (j = 2, 3, \ldots, 36) \tag{A-5b}$$

where Θ is the dimensionless number defined as

$$\Theta = y_{in}F/u_y V \tag{A-6}$$

Substituting $j = 36$ into Eq. (A-5b) yields

$$\overline{C_{36}}(t_1) = \frac{\exp(-35\Theta) - \exp(-36\Theta)}{1 - \exp(-36\Theta)} \tag{A-7}$$

and the concentration in the chambers can be expressed as

$$\frac{\overline{C_j}}{C_0} = 1 - \alpha \exp\left(-\frac{t}{\tau}\right) \qquad (j = 1) \tag{A-8a}$$

$$= \{\exp[-(j-2)\Theta] - \alpha \exp[-(j-1)\Theta]\} \exp\left(-\frac{t}{\tau}\right) \qquad (j = 2, 3, \ldots, 36) \tag{A-8b}$$

Here,

$$\alpha = \frac{C_0 - \overline{C_{36}}(t_1)}{C_0} = \frac{1 - \exp(-35\Theta)}{1 - \exp(-36\Theta)} \tag{A-9}$$

The solute concentration at the inlet boundary of the packed bed is equal to that in the inlet chamber and varies periodically. In order to simplify the mathematical treatment, let us take the time average of the equation over one time cycle and derive the steady-state boundary equation for the annular column inlet.

In Fig. 4, the chamber upon a point y in $0 < y \leq y_{in}$ is the second and first during $0 \leq t \leq y/u_y$ and $y/y_y < t \leq t_1$, respectively. Over the time interval $0 \leq t \leq t_1$, the average concentration at point y can be given as Eq. (1-a). Similarly the $(j+1)$th and jth chambers are located upon a point y in $y_{in} < y \leq 35y_{in}$ over the time interval $0 \leq t \leq \{y - (j-1)y_{in}\}/u_y$ and $\{y - (j-1)y_{in}\}/u_y < t \leq t_1$, respectively, and the average

concentration can be given as Eq. (1-b). The first and the 36th chambers are located upon a point y between $35y_{in} < y \leq 36y_{in}$ over the time average $0 \leq t \leq (y - 35y_{in})/u_y$ and $(y - 35y_{in})/u_y < t \leq t_1$, respectively, and the average concentration can be given as Eq. (1-c).

NOMENCLATURE

C	concentration (mol/m^3)
$\overline{C}$	integral average concentration (mol/m^3)
C_0	concentration in feed solution (mol/m^3)
$\overline{C_j}$	concentration at the jth inlet chamber (mol/m^3)
E_y	circumferential dispersion coefficient (m^2/s)
E_z	axial dispersion coefficient (m^2/s)
F	volumetric flow rate (m^3/s)
L	height of separation tower (m)
t	time (s)
t_1	time interval for feed concentration for inlet compartment, y_{in}/u_y (s)
u_y	tangential velocity (m/s)
u_z	interstitial fluid velocity (m/s)
V	liquid volume in the inlet chamber (m^3)
y	circumferential coordinate (m)
y_{in}	width of inlet chamber (m)
z	axial coordinate (m)

Greek

α	dimensionless group defined in Eq. (A-9) (—)
Θ	dimensionless group defined in Eq. (13) (—)
ω	angular velocity (rad/s)

Subscript

j	number of the inlet chamber

REFERENCES

1. A. J. P. Martin, *Discuss. Faraday Soc.*, *7*, 332 (1949).
2. J. C. Giddings, *Anal. Chem.*, *34*, 37 (1962).
3. J. B. Fox, R. C. Calhoun, and W. J. Eglinton, *J. Chromatogr.*, *43*, 48 (1969).
4. J. B. Fox, *Ibid.*, *43*, 55 (1969).
5. R. A. Nicholas and J. B. Fox, *Ibid.*, *43*, 61 (1969).
6. J. M. Begovich and W. G. Sisson, *Resour. Conserv.*, *9*, 219 (1982).
7. J. M. Begovich and W. G. Sisson, *AIChE J.*, *30*, 705 (1984).

8. M. Goto and S. Goto, *J. Chem. Eng. Jpn.*, *20*, 598 (1987).
9. A. J. Howard, G. Carta, and C. H. Byers, *Ind. Eng. Chem. Res.*, *27*, 1873 (1988).
10. K. Hashimoto, M. Morishita, S. Adachi, K. Shindo, Y. Shirai, and M. Tanigaki, *Prep. Chromatogr.*, *1*, 163 (1989).
11. C. L. Ligny, *Chem. Eng. Sci.*, *25*, 1177 (1970).

Received by editor December 11, 1992
Revised May 17, 1993